Calibration of gas flow meters using choked flow and an evacuated vessel

Max B Trueblood[1,6,*] , **Otmar Schmid**[2], **Nicholas Altese**[1], **Christian J Hurst**[1], **Wenyan Liu**[4,5], **Teresa Gelles**[3], **Steven C Achterberg**[1], **Philip D Whitefield**[1,5] **and Donald E Hagen**[1]

[1] Center of Excellence for Aerospace Particulate Emissions Reduction Research, Missouri University of Science and Technology, Rolla, MO 65409, United States of America
[2] Institute of Lung Biology and Disease, Helmholtz Zentrum Munchen—German Research Center for Environmental Health, Ingolstaedter Landstrasse 1, Neuherberg 85764, Germany
[3] Chemical Engineering Department, Missouri University of Science and Technology, Rolla, MO 65409, United States of America
[4] Department of Chemistry, Missouri University of Science and Technology, Rolla, MO 65409, United States of America
[5] Center for Research in Energy and Environment, Missouri University of Science and Technology, Rolla, MO 65409, United States of America
[6] Lasea Aerosol Services, Ltd, 14075 St Rt Y, Rolla, MO 65401, United States of America

E-mail: trueblud@umsystem.edu

CrossMark

Abstract

The measurement of gas flow rates is of great importance in a wide range of modern technologies. This paper introduces a simple, yet accurate technique for in-house calibration of gas FMs (mass and volumetric) even under harsh environmental conditions such as encountered during field measurement campaigns. The method requires only readily available, low cost components: a vessel of known volume, an air pump, a pressure sensor and a metal plate orifice or a needle valve to act as a CO. The unique property of choked flow in the CO is used here for flow calibration. In the method presented here a vessel is evacuated to below the critical pressure (<0.53 of upstream pressure) and then allowed to refill with ambient air (or some other process gas) under so-called *choked flow* conditions through the CO. The method presented here leverages that the flow rate upstream of the CO is not only constant but readily determined from (a) the known V_{VESS}, (b) the measured time rate of change of the absolute pressure in the vessel and (c) the ideal gas law. This calculated flow rate can be used for calibration of FMs. The accuracy of the method depends only on the accuracy of the pressure measurement, the timer and the value of the V_{VESS}. The flow rate computed in this way is found to be in excellent agreement (typically 1% difference) with the flow rate measured by a soap film FM (Gilibrator). As expected from theory this method is found to work for all kinds of CFRs (here: various types of metal plate orifices and needle valves were tested), gas types (here: air, Argon, and CO_2) and upstream pressures (here: between 650 hPa and 1400 hPa). The accuracy of this technique

* Author to whom any correspondence should be addressed.

(~1%) is as good as that of standard volume displacement methods (e.g. soap film FMs) (typically 1% difference), the standard of laboratory-based flow calibrators, but less expensive and more suitable for harsh environments.

(Some figures may appear in color only in the online journal)

Nomenclature

$B_{FMrefstd}$	Y-intercept of the $Q_{FMrefstd}$ vs output voltage V_{fm} of the flowmeter
CFEV	Choked flow evacuated vessel
CO	Critical orifice
CFR	Choked flow restrictor or critical flow restrictor
C_p	Constant pressure specific heat (J K^{-1})
C_v	Constant volume specific heat (J K^{-1})
d	Orifice diameter (units indicated in table)
DMA	Differential mobility analyzer
dt	Elapsed time (s)
dn/dt	Time rate of change of number of moles of gas in the vessel (mol min^{-1})
dP_{dn}/dt	Time rate of change of pressure in the vessel (hPa sec^{-1})
FM	Flow meter
FM$_{ref}$	Reference flow meter
HHPA	House high pressure air
LV01	LabVIEW program that collected data
MFM	Mass flow meter
MKS$_{1179}$	The MKS mass flow meter, model number 1179
$M_{FMrefstd}$	Slope of the plot of Q$_{FMrefstd}$ vs V_{fm}
M_{Pdn}	Slope of plot of P_{dn} vs elapsed time dt (hPa s^{-1})
n	Moles of gas (mol)
P	Pressure (hPa)
P_{ratio}	Ratio of (P_{dn}/P_{up}) (unitless)
P_{crit}	Critical pressure ratio (unitless)
P_g	Pressure of the gas near the Gilibrator (hPa)
P_{dn}	Orifice downstream pressure (hPa)
P_{up}	Orifice upstream pressure (hPa)
P_{std}	Standard pressure (1013 hPa)
P_{1up}	Pressure upstream of the reference flow meter
$Q_{FMrefstd}$	Gas flow rate through the reference flow meter (SL min^{-1})
Q_{GIL}	Gas flow rate from Gilibrator, not adjusted to standard conditions (L min^{-1})
Q_{GILstd}	Gas flow rate from Gilibrator, converted to standard conditions (SL min^{-1})
$Q_{CFEVstd}$	Gas flow rate from choked flow evacuated vessel technique (SL min^{-1})
Q$_2$	Excess flow out of the system (L min^{-1})
Q_{VFMup}	Volumetric flow rate upstream of the VFM (L min^{-1})
Q_{VFMdn}	Volumetric flow rate downstream of the VFM (L min^{-1})
R	Ideal gas law constant (8.314 J mol^{-1} K^{-1})
Re	Reynolds number (dimensionless)
dt	Elapsed time (s)
T	Temperature (K)
T_{dn}	Temperature downstream of the critical orifice (K)
T_{up}	Temperature upstream of the critical orifice (K)
T_{1up}	Temperature upstream of the reference flow meter
T_g	Temperature of the gas near the Gilibrator (K)
T_{std}	Standard temperature (273.15 K)
V	Volume of a gas (l)
V_{vess}	Vessel volume (l)
V_{fm}	FM output signal (V_{dc}) from either an MFM or a VFM
VFM	Volumetric flow meter

Greek symbols

β	Orifice to pipe diameter ratio, dimensionless
γ	Heat capacity ratio (dimensionless)

1. Introduction

An accurate means of determining the flow rate of gases underlies many commercial, research and regulatory activities. One important example is the understanding and eventual regulation of the emissions associated with commercial aviation. As air travel increases, the impact of aviation on local air quality (Levy *et al* 2012) and climate has drawn significant attention (Waitz *et al* 2004, Lee *et al* 2009, 2010, EASA 2015). Accurate measurements of the concentrations of these emission species (particulate matter and gases) can be achieved using extractive flow sampling which requires an accurate means of measuring the flow rates of these species and their carrier gases. Many field campaigns designed to measure the effluents from gas turbine engines and rocket engines have been conducted over the last 30 years (Bulzan *et al* 2010, Christie *et al* 2012, Hagen *et al* 1992, 1997, 1999, Kinsey *et al* 2010, 2012, Lobo *et al* 2011, 2012, 2015, Moore *et al* 2017, Paladino *et al* 2000, Ross *et al* 1999, 2000, Schulte *et al* 1997, Trueblood *et al* 2018, Whitefield *et al* 1999).

There are several different types of gas FMs on the market (Baker 2016). These include MFMs (ones that use heating elements and temperature sensors, ones that use the Coriolis effect, etc) and VFMs (ones that measure the pressure drop across a laminar flow element, soap film FMs, rotameters, etc). The method presented here can be used to calibrate any type of FM.

Several methods for calibrating FMs are described in the literature. These are

(a) the soap film prover (Waaben *et al* 1978, Lashkari and Kruczek 2008);

(b) the piston prover (Wright and Mattingly 1998a, Wright *et al* 1998b);

(c) the bell prover (Wright and Mattingly 1998a, Wright 1998c, Paton 2005);

(d) the critical flow venturi nozzle is a meter with very high measurement accuracy and is used for testing, calibration and flow control. This device is such that if it is machined in accordance with the design and the pressure and temperature upstream are controlled, it will produce the specified flow. Considerable effort has been devoted to characterizing critical flow nozzles and how they can produce known, predictable flow for a certain geometry and upstream pressure (Johnson *et al* 1998). Although we make use of COs in this paper, they are not used in that way–we do not make use of their design to predict what the flow through them is;

(e) the most prominent and trusted method seems to be the pressure, volume, temperature and time method (PVTt). Over a period of several decades, several laboratories have developed their apparatuses that use this method (Kegel 1995, Wright and Mattingly 1998a, Wright *et al* 2004, Nakao 2006, Johnson and Wright 2009, Mascomani and Chandapillai 2017).

Additional efforts have been spent to compare the apparatuses from different national metrology labs, where at least one of them was the PVTt apparatus (Wright *et al* 1998b).

Although our technique is quite similar to the PVTt method, there are some major differences. One difference is that it appears that the PVTt method has the gas entering the calibration apparatus at a pressure significantly higher than one atmosphere (at least for some calibrations), since they mention the increase in temperature of the gas as it enters the capturing tank or vessel and is compressed (Wright and Johnson 2000). Thus, the capturing vessel must be immersed in a temperature controlled water bath. Since the gas entering our calibration facility is only at room pressure and only enters the capturing vessel at less than one half an atmosphere, there is no increase in temperature and no need to immerse the vessel in a temperature controlled bath.

A second difference is that the PVTt method takes only two measurements of pressure and temperature. One is at the beginning of the filling and one is at the end. Our method requires measuring the gas pressure at 1 Hz.

A third difference is that in the PVTt method, they calculate the density of the gas in the vessel using an actual equation of state which has the compressibility coefficient for that gas incorporated into the ideal gas law. The mass of the gas is then computed from the gas density and known tank volume. It may well be that the PVTt method is more all encompassing than ours, because it takes into account the compressibility of the gas. However, our technique worked quite well for the gases we tested. Alternatively, it could well be that if we incorporated the gas compressibility coefficient into our ideal gas law equation (equation (4)), we would also be able to use many other gases. Perhaps that is work for another paper.

Levine (2010) proposed a sophisticated technique very similar to ours (also giving predicted accuracy), but as far as we can tell never built the apparatus nor published any results. As will be seen later, unlike the Levine description, our method requires almost no special equipment to yield quite accurate results.

Most of these other methods either provide very high accuracy and precision and/or involve an apparatus that requires tight temperature control in a laboratory or having the tanks submerged in a temperature controlled water bath. In the absence of an in-house standard, a user's FM must be returned to the manufacturer for recalibration, which can prove time consuming and costly to the user. Also, sometimes it is necessary to use a FM with a gas for which it was not calibrated. For example, Schmid *et al* (2010) showed how to successfully operate a DMA, which relies on accurate measurement of the flow rate of the sample and sheath flow, with gases other than air (He, Ar, H_2, CO_2, and N_2O). Therefore, a simple, inexpensive, yet accurate technique for calibrating a gas FM for any type of gas seems desirable.

Good laboratory practice dictates that electronic devices (such as gas FMs) be calibrated yearly. The method presented here involves pieces of equipment that many laboratories already have on hand, thus making it possible for the typical laboratory personnel to calibrate their own gas FMs whenever it is desired. This study presents a simple, inexpensive, yet accurate method for calibration of gas FMs utilizing the unique properties of a CO, the CFEV method.

The experimental setup, the principle of operation and the governing equations are described. The validity of the method is established by comparison with a soap film FM (an accepted standard for flow rate measurements) and its wide range of applicability is demonstrated by using different types of COs, gas types and pressure conditions.

2. Theory

2.1. Critical pressure ratio across an orifice

The fundamental concept of generating a constant volumetric flow rate by operating an orifice under critical pressure conditions (choked flow) relies on the fact, that—except for specially designed nozzles—the flow velocity through a nozzle is limited by the speed of sound. Any orifice becomes critical once the ratio of downstream and upstream pressure falls below a certain, critical value (Perry and Chilton 1973). Cunningham (1951) seems to imply that the flow rate does not remain constant over the entire range of $0 < P_{dn}/P_{up} < 0.45$. We did not observe any such change in the flow rate. Assuming a perfect gas, a frictionless orifice, defining β as the ratio of the orifice diameter to pipe diameter, and if $\beta \leqslant 0.2$ then the critical pressure ratio is given by

$$\left(\frac{P_{dn}}{P_{up}}\right)_{crit} = \left(\frac{2}{\gamma+1}\right)^{\left(\frac{\gamma}{\gamma-1}\right)} \tag{1}$$

where $\gamma \ (= C_p/C_v)$ is the ratio of the heat capacities of the gas under constant pressure and volume conditions, respectively.
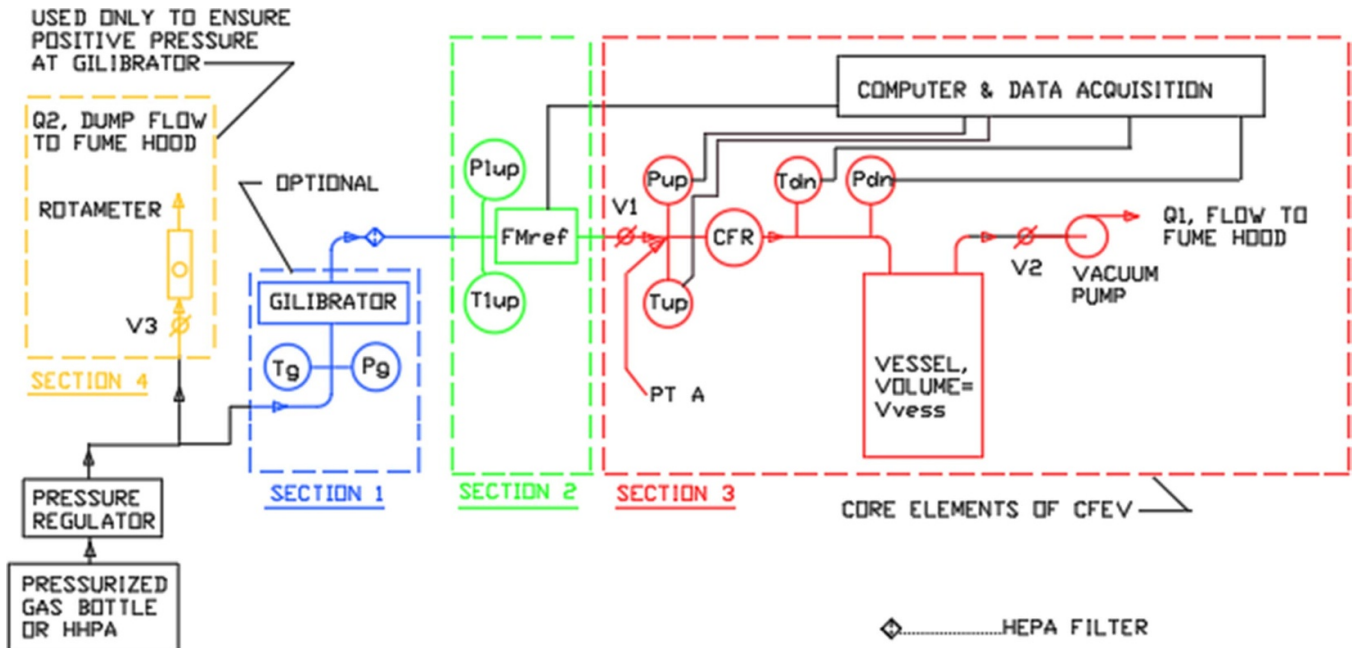
Figure 1. Schematic of the apparatus used to validate the CFEV method with a calibrated FM$_{ref}$ or with a soap film FM (Gilibrator).

For air with $\gamma = 1.4$ the critical pressure ratio becomes

$$\left(\frac{P_{dn}}{P_{up}}\right)_{crit} = 0.528 \, (\text{for air}). \tag{2}$$

Critical pressure ratios for other gases are, e.g. 0.547 for CO_2 ($\gamma = 1.289$) and 0.487 for Argon ($\gamma = 1.667$).

2.2. Obtaining the reference flow rate for FM calibration using the CFEV method

As mentioned above, as long as the pressure drop across an orifice is larger than the critical pressure ratio (i.e. $P_{ratio} = P_{dn}/P_{up} < P_{crit}$) the upstream volumetric flow rate is fixed to a certain value which does not depend on the absolute pressure downstream of the orifice (Perry and Chilton 1973). Most of the commonly used gases (air, argon, nitrogen, CO_2, etc) can be well approximated as ideal gases except in the limits of extremely low temperature or high pressure, which is irrelevant for most applications. A schematic of the apparatus is given in figure 1. For an evacuated vessel which is gradually refilled through a CFR, the volumetric gas flow rate into the vessel is related to the observed rate of pressure change in the vessel. The experimental details will be described below. First, fundamental equations used for determination of the flow rates as computed from the CFEV method from the measured parameters are derived.

According to the ideal gas law,

$$n = \frac{V}{RT}P. \tag{3}$$

The rate equation for molar gas flow into the vessel can be expressed as

$$\left(\frac{dn}{dt}\right) = \frac{V_{vess}}{RT_{dn}}\left(\frac{dP_{dn}}{dt}\right) \tag{4}$$

where n is the number of moles of gas in the vessel, R is the ideal gas law constant (8.314 J mol^{-1} K^{-1}), V_{vess}, P_{dn} and T_{dn} are the volume of the vessel, the pressure and temperature in the vessel, respectively, and t is the elapsed time. Since the molar gas flow rate is conserved (in the absence of leaks or gas sources), the molar flow rate into the vessel is the same as the flow rate through the Gilibrator and the flow meter (FM$_{ref}$). Equation (4) implies that the volume of the apparatus (V_{vess}) and the temperature of the gas upstream and downstream of the orifice are constant. The former is obvious and the latter is a characteristic of ideal gases. That is, as the gas velocity increases in the narrow constrictions (orifice), the increase in kinetic energy is matched by an adiabatic cooling of the gas. For ideal gases, this conversion of energy is reversible, i.e. the cooling is reversed once the gas slows down upon exiting the orifice. Thus there is no difference between upstream and downstream gas temperature (the temperature of the gas downstream of the orifice was measured and found to be only 0.1 °C different from the temperature of the gas upstream of the orifice).

Although some researchers (Wright and Johnson 2000) do, in fact, see an increase in gas temperature of as much as 10 K, we do not observe that. It appears that they are filling their vessel to a higher pressure than we do, thus doing work on the gas.

The molar flow rate (dn/dt) is equivalent to the mass flow rate (using the molar mass), which is typically expressed as volume flow rate for certain reference temperature and pressure conditions. At standard temperature ($T_{std} = 273.1$ K) and pressure ($P_{std} = 1013$ hPa), one can rewrite equation (4) into

$$\left(\frac{dn}{dt}\right) = \frac{V_{\text{vess}}}{RT_{\text{dn}}} \cdot \left(\frac{dP_{\text{dn}}}{dt}\right) = \frac{V_{\text{vess}}}{T_{\text{dn}}} \cdot \frac{\text{K mol}}{8.314\,\text{J}} \cdot \frac{\text{J}}{\text{N m}} \cdot \frac{22.4\,\text{SL}}{1\,\text{mol}}$$
$$\cdot \frac{100\,\text{Pa}}{1\,\text{hPa}} \cdot \frac{1\,\text{N}}{1\,\text{Pa} \cdot \text{m}^2} \cdot \frac{1\,\text{m}^3}{1000\,\text{l}} \cdot \frac{60\,\text{s}}{1\,\text{min}} \cdot \left(\frac{dP_{\text{dn}}}{dt}\right)$$

$$\left(\frac{dn}{dt}\right) = Q_{\text{CFEVstd}}\left(\text{SL min}^{-1}\right) = 16.165 \cdot \frac{V_{\text{vess}}\,(\text{l})}{273.15 + T_{\text{dn}}\,(\text{C})}$$
$$\cdot \frac{dP_{\text{dn}}}{dt}\left(\text{hPa s}^{-1}\right) \qquad (5a)$$

where Q_{CFEVstd} is in SL min^{-1}, V_{vess} is in liters, and dP_{dn}/dt is in hPa s^{-1}.

We note in passing that some (but not all) organizations have changed their definition of standard atmospheric pressure (McNaught and Wilkinson 1997). The temperature T_{dn} (in °C) can be measured anywhere (except in the orifice) and for simplicity even ambient air temperature can be used, if the apparatus is in thermal equilibrium with the ambient air.

For calibration of VFMs, allowance must be made for the pressure and temperature at the point where the flow is desired. Hence, the volumetric flow rate downstream of the VFM is

$$Q_{\text{VFMdn}}\left(\text{l min}^{-1}\right) = Q_{\text{CFEVstd}} \cdot \left(\text{SL min}^{-1}\right) \cdot \left(\frac{P_{\text{std}}}{P_{\text{up}}}\right)$$
$$\cdot \left(\frac{T_{\text{up}}}{T_{\text{std}}}\right). \qquad (5b)$$

The volumetric flow rate upstream of the VFM is given by

$$Q_{\text{VFMup}}\left(\text{l min}^{-1}\right) = Q_{\text{CFEVstd}} \cdot \left(\text{SL min}^{-1}\right) \cdot \left(\frac{P_{\text{std}}}{P_{1\text{up}}}\right)$$
$$\cdot \left(\frac{T_{1\text{up}}}{T_{\text{std}}}\right) \qquad (5c)$$

where P_{up}, $P_{1\text{up}}$, T_{up} and $T_{1\text{up}}$ are measured at the positions indicated in figure 1. In contrast to MFMs, the volume flow rate depends on pressure and temperature, i.e. if there is a pressure and/or temperature change across the VFM to be calibrated, this has to be corrected for as described in equations (5b) and (5c).

3. Experimental

3.1. Reference flow meter

In order to validate the present technique, a direct comparison of the flow rate as given by the CFEV method with the flow rate as given by some reference or standard FM had to be performed. In this study, a soap film FM was used as the reference device. Soap film FMs (or other volume displacement devices) are primary measurement devices, which measure the displaced gas volume per time.

Although it is shown in figure 1, for practical and technical reasons the soap film FM (figure 1, section 1, blue) (Gilibrator-2, Sensidyne LP, 1000 112th Circle North, Suite 100, St. Petersburg, FL 33716, USA) could not be used as the standard or reference flowmeter in all the experiments described in this study. (It was, however, utilized for some experiments). This

is because (a) obtaining measurements with a Gilibrator takes much longer than with an electronic FM and (b) the Gilibrator is not suitable for pressures much larger or smaller than ambient pressure. Therefore, we first (see figure 2) deployed the Gilibrator to calibrate an electronic (thermal) MFM (figure 1, section 2, Green) (MKS MN 1179; powered and monitored by an MKS 247-D, MKS Instruments, 2 Tech Drive, Suite 201, Andover, MA 01810, USA) with 20 SL min^{-1} full scale. This MKS$_{1179}$ was then used as the FM$_{\text{ref}}$. The Gilibrator is itself factory calibrated once per year, as recommended by the manufacturer, who provides a certificate of calibration. The calibration sheet from Sensidyne LP states that the 'calibration was performed using standards and instruments that are traceable to the International System of units (SI) through the National Institute of Standards and Technology (NIST)'.

For all discussion, results, and experimentation described in this paper, the FM$_{\text{ref}}$ shown in figure 1 was a MFM, MKS$_{1179}$, which was periodically calibrated by the Gilibrator (see figure 2). Once this CFEV technique is accepted by others, they can then place their gas FM in the place of FM$_{\text{ref}}$ in figure 1 (section 2) and use the CFEV method to calibrate their gas FMs, without the Gilibrator (section 1, of figure 1).

When calibrating the reference MFM (FM$_{\text{ref}}$) with air, compressed air from HHPA was used, rather than room air and a pump. This was for the sake of consistency (HHPA had a consistently low relative humidity) and to avoid pump-associated pressure pulses, which might adversely affect the accuracy of the FM$_{\text{ref}}$ calibration. The flow rate was adjusted using valves V1 and/or V2. Since the flow cell of the Gilibrator can only be operated near ambient pressure conditions, valve V3 and the pressure regulator were adjusted to provide a small excess gas flow Q_2, as registered by the rotameter. The positive flow Q_2 ensured that the pressure at the Gilibrator was only slightly above ambient pressure and the gas being supplied to the calibration apparatus was, in fact, coming from the intended source. Although the pressurized gas bottle/pressure regulator can exert a substantial pressure, the Gilibrator cannot operate at pressures much above one atmosphere (say 30 hPa). Hence, the vacuum pump and valves V_1 and V_2 are required to pull gas flow through the system.

The temperature T_{g} and pressure P_{g} of the gas entering the Gilibrator were measured by a thermistor thermometer (MN 5831, Omega Engr, Stamford, CT 06907, USA) and a precision pressure gauge (MN 15000, Mensor Corp, 201 Barnes Dr, San Marcos, TX 78666, USA), respectively. The signals from the pressure probes and FM$_{\text{ref}}$ were collected by a LabVIEW program (LV01) utilizing a USB-6009 (National Instruments, 11500N Mopac Expwy Austin, TX 78759-3504) and laptop computer. The volumetric flow rate of the Q_{GIL} (L min^{-1}) was converted into standard flow rate ($P_{\text{std}} = 1013$ hPa and $T_{\text{std}} = 273.2$ K) according to

$$Q_{\text{GILstd}} = Q_{\text{GIL}} \frac{P_{\text{g}}}{P_{\text{std}}} \cdot \frac{T_{\text{std}}}{T_{\text{g}}}. \qquad (6)$$

The standard flow rate as computed from the Gilibrator Q_{GILstd} can then be related to the FM$_{\text{ref}}$ output signal (V_{fm}) (0–5 V) yielding coefficients of a linear calibration curve
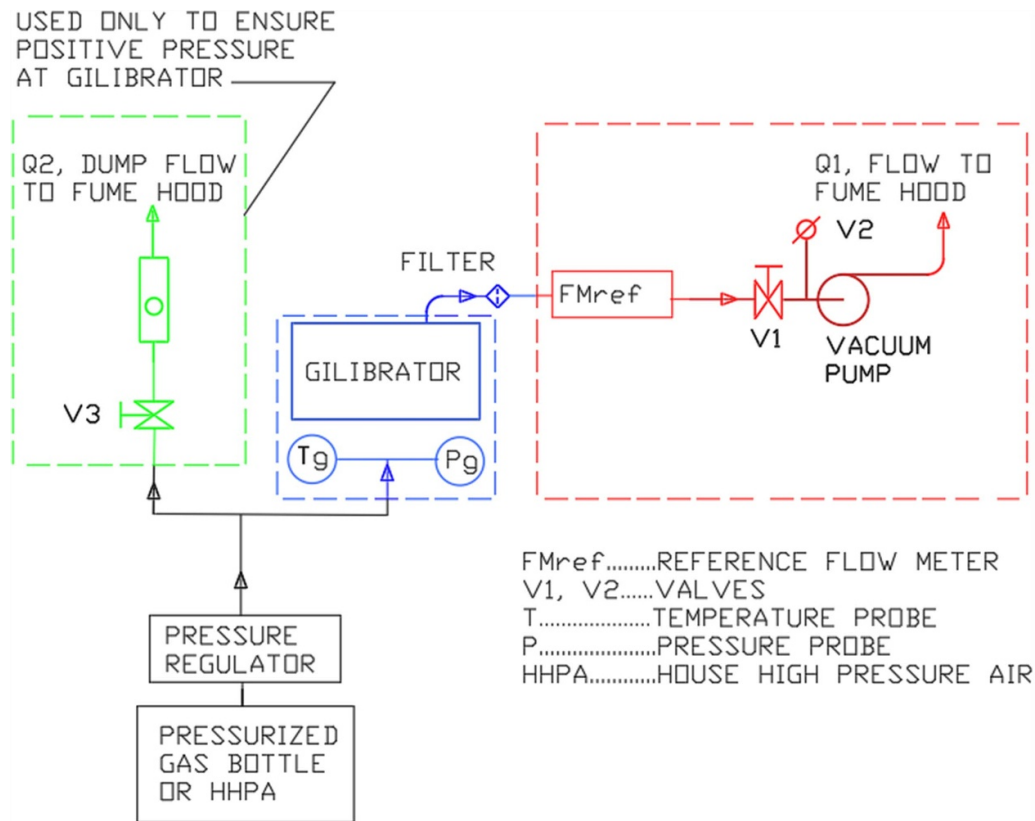
Figure 2. Schematic of the apparatus used to calibrate a reference MFM FM$_{ref}$ using the Gilibrator. The flow through the system was regulated with valves V1 and/or V2. The use of pressurized gas bottles as gas supply guarantees the absence of pump-induced pressure pulses, which might affect the accuracy of the calibration. V3 ensures a slight positive pressure on the rest of the system.
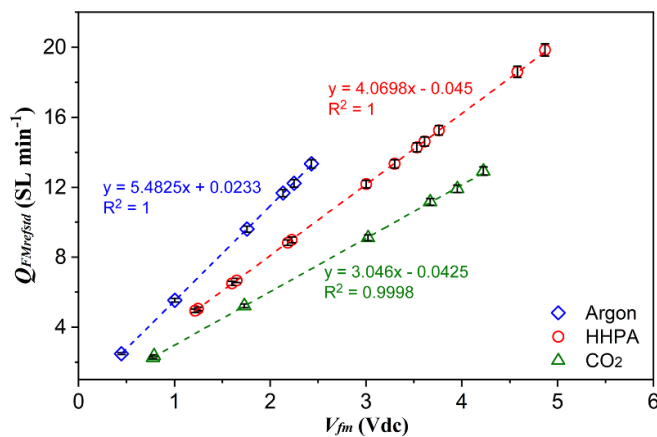
Figure 3. $Q_{FMrefstd}$ vs FM$_{ref}$ output voltage V_{fm} for three different gases.

$$Q_{FMrefstd} = Q_{GILstd} = M_{FMrefstd} \times V_{fm} + B_{FMrefstd}. \quad (7)$$

The same calibration was done for argon and CO_2 as operating gases. Since the measurement principle of thermal MFMs depends on gas type (heat capacity and thermal conductivity of the gas), the calibration curves depend on gas type as seen from figure 3.

The V_{vess} was determined by weighing the mass of deionized water required to fill it. Deionized water was drawn into four 5 gallon buckets and allowed to temperature equilibrate for one day, so that the water and the vessel in our apparatus were both at room temperature. The sliding mass balance was calibrated with weights borrowed from the Missouri Department of Agriculture's Metrology Lab (1616 Missouri Boulevard, Jefferson City, MO 65102). These weights were certified to have an accuracy of 0.01%. The volume of that mass of water was then temperature corrected (Jones and Harris 1992). This measurement was performed three times resulting in an average V_{vess} of 62.721 l and a standard deviation of 0.012 l.

Studies published using the PVTt method mention the 'inventory volume' of their apparatus. This is the volume of the tubing between the CO and the collection vessel. In our apparatus, the inventory volume was 0.018 l (or 0.0003 of the V_{VESS}). Our inventory volume was considered as part of the V_{VESS}, since it and the vessel are at the same temperature and pressure for the filling process.

Wright *et al* (2004) considered how much their tank expands as the pressure in it increases. It is our understanding that in their apparatus, the final pressure might be well above one atmosphere. Since our tank volume was measured at 1 atm and room temperature, and the final pressure of the tank was 1/2 atm and room temperature, we do not believe a correction is necessary.
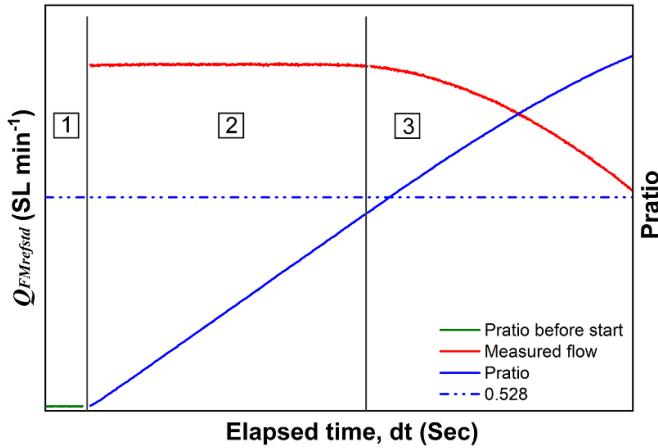
Figure 4. The pressure P_{dn} (green) before allowing flow into the vessel, the flow rate $Q_{FMrefstd}$ (red) while allowing flow into the vessel, and the pressure ratio ($P_{ratio} = P_{dn}/P_{up}$) (blue) vs elapsed time dt. Notice that during phase 2, while the flow is choked, the flow is very constant, i.e. up until the critical pressure ratio of approximately 0.5.

3.2. Principle of operation of the CFEV method

Figure 1 shows the experimental apparatus for the CFEV technique of calibrating an FM. The process of FM calibration with the CFEV method can be divided into three phases readily identifiable by the pressure ratio ($P_{ratio} = P_{dn}/P_{up}$) (figure 4). Here, a LabVIEW program (LV01) is used for data acquisition and real-time conversion of the voltage signals into flow rates (according to equations (5) and (7)) and pressures. Pressure transducers P_{up} and P_{dn} monitor the pressures upstream and downstream of the CFR. Transducers P_{up} and P_{dn} were Omega, PX 138-030A5V, 0–30 psia (Omega Engineering, Inc. 800 Connecticut Ave., Suite 5N01, Norwalk, CT 06854). They were calibrated against a pressure standard (MN 15000 mentioned above). This pressure standard is also returned to the factory once per year for factory calibration, and the factory provides a certificate of calibration.

To begin, the gas source is adjusted so that the excess flow Q₂ is approximately 5 l min⁻¹ greater than what will be required for the next intended data point. Ball valve V1 is closed, ball valve V2 is opened and the vacuum pump is allowed to evacuate the vessel far below the critical P_{ratio} ($\ll 0.53$; here ca. 0.01, i.e. $P_{dn} \sim 10$ hPa). Then V2 is closed and the P_{dn} remains at this value, since V1 is closed. As a measure of quality control P_{dn} is observed for approximately 60 s to confirm that there are no leaks (constant P_{dn} value) (phase 1 in figure 4).

Then V1 is opened (phase 2 in figure 4) and gas gradually flows via the FM$_{ref}$ and CFR into the evacuated vessel resulting in a gradual, linear rise of P_{ratio} and a constant flow rate, which depends on the type and settings of the CFR (figure 4). As long as the orifice is critical, the flow rate is constant as verified by the FM$_{ref}$ signal (V_{fm}), and P_{dn} increases at a constant rate. Phase 2 is the region used for FM calibration with the CFEV method.

As the vessel fills, the pressure ratio ($P_{ratio} = P_{dn}/P_{up}$) approaches 0.528 and the flow rate of the gas passing PT A

as measured by the FM$_{ref}$ is constant. Phase 2 ends when the flow through the FM$_{ref}$ ($Q_{FMrefstd}$) drops ever so slightly, say by 1% or so.

Phase 3 is the period during which the gas flow is no longer choked. During phase 3, the pressure ratio will continue to increase to its asymptotic value of unity and the flow as measured by the $Q_{FMrefstd}$ will continue to decrease to its asymptotic value of zero (not shown). Typically, LV01 was allowed to gather data for another 60 s or so, then data logging was terminated.

The LabVIEW program (LV01) produced a text file with columns for elapsed time (dt), the raw voltages from each of P_{up} and P_{dn}, the pressures corresponding to those signals, the raw voltage from the FM$_{ref}$ (V_{fm}) and the flow computed from that FM$_{ref}$ reading using equation (7). This flow was obtained from the previous calibration of the FM$_{ref}$ using the Gilibrator (figure 2). A plot of P_{dn} vs dt was generated and a linear regression was used to fit a straight line to the data, i.e.

$$P_{dn}\,(hPa) = M_{Pdn}\,(hPa\,s^{-1}) \cdot dt\,(s). \tag{8}$$

The slope $M_{P_{dn}}$ (dP_{dn}/dt) from equation (8) is used in equation (5) to obtain the flow $Q_{CFEVstd}$ (SL min⁻¹) past Pt A and into the vessel

$$Q_{CFEVstd}\,\left(SL\,min^{-1}\right) = 16.165 \cdot \frac{V_{vess}\,(l)}{273.15 + T_{dn}\,(C)} \cdot M_{P_{dn}}\,\left(hPa\,s^{-1}\right). \tag{9}$$

The goal of the present study is to show the validity of calibrating a FM using the CFEV. Thus, we compare $Q_{CFEVstd}$ from equation (9) to the average value of $Q_{FMrefstd}$ from equation (7) (computed every 1 s by LV01 and logged in the data file) or to the average of the Gilibrator (Q_{GILstd}) equation (6) (taken several times manually) for the time period when the orifice was critical (phase 2).

It is important to realize that once the FM$_{ref}$ is calibrated using the setup in figure 2, then there are three sections of the apparatus shown in figure 1 that can each provide a measure of the gas flow rate (sections 1, 2 or 3 of figure 1). Once the FM$_{ref}$ (i.e. MKS$_{1179}$) has been calibrated with the Gilibrator as in figure 2, then effectively there is a standard FM in figure 1, be it the FM$_{ref}$ (the calibrated MKS$_{1179}$) or the Gilibrator itself. For all of the experiments performed in this study, the gas flow as calculated from the CFEV method (section 3) was compared to the gas flow as measured by the Gilibrator (section 1) or the Gilibrator calibrated FM$_{ref}$ (the MKS$_{1179}$) (section 2).

Once an investigator accepts the validity of the CFEV method, then he/she may install his/her own FM into section 2 and use section 3 as the reference flowmeter and calibrate his/her FM against it.

The present method is fairly similar in principle to the method used by the US NIST Fluid flow Group, what they refer to as the pressure, volume, temperature, time (PVTt) method (Wright *et al* 2004). In the PVTt method, the gas is passed through the flowmeter to be calibrated, a CFR, and then allowed into an evacuated vessel, which is immersed in a temperature controlled water bath. The initial and final pressure and temperature of the gas in the vessel are measured.

Table 1. Characteristics of the O'Keefe orifices.

Catalogue number	Orifice diameter, d (cm)	Observed P_{ratio} limit	Flow rate $Q_{FMrefstd}$ (SL min^{-1})	Flow rate $Q_{CFEVstd}$ (SL min^{-1})	Relative difference $Q_{FMrefstd}$ and $Q_{CFEVstd}$
K6-26-SS	0.0660	0.493	3.035	3.010	0.008
K6-38-SS	0.0965	0.528	6.756	6.706	0.007
K6-52-SS	0.1321	0.479	11.69	11.60	0.008
K6-60-SS	0.1524	0.518	14.14	14.16	−0.001
K6-63-SS	0.1600	0.524	15.32	15.41	−0.006
K6-67-SS	0.1702	0.498	16.14	16.11	0.002

Only the time interval for the entire vessel filling is measured, i.e. a beginning and an ending time. The test gas in the vessel is allowed several minutes to come to temperature equilibrium with the temperature controlled bath. The mass of the gas allowed into the tank is determined by knowing the pressure and temperature of the gas in the tank. Rather than using the ideal gas law (as we do), they use an actual equation of state that is identical to the ideal gas law, except it incorporates the compressibility factor for that particular gas (Wright *et al* 2004). Thus the PVTt method is perhaps more all inclusive, capable of calibrating FMs with a wider range of gases. Indeed, the PVTt method is the recognized worldwide standard. Workshops have been conducted wherein the US NIST PVTt apparatus has been compared to that of other nations (Wright *et al* 1998b).

It is important to realize, however, that for many experimenters who want to calibrate their own flowmeters quickly, accurately, inexpensively, and without having to send the flowmeter off for an extended period of time, our method is quite adequate for gases that are approximated by the ideal gas law.

4. Metal plate orifices as the CFRs

For the first part of this set of experiments, metal plate orifices (table 1) designed for controlling airflow (O'Keefe Controls, 4 Maple Drive, Monroe, CT 06468) were utilized as the CFRs to cause constant gas flow through the FM$_{ref}$. The metal plate orifices were in the form of stainless steel cylinders 57.7 mm in length and 9.5 mm in outside diameter. Figure 5 (an actual data plot) displays real data taken using a metal plate orifice that is similar to figure 4 (the idealized plot). It is important to emphasize that absolutely every experiment performed for this study produced a plot completely similar to figure 5. That is, the gas flow measured by the reference flowmeter was very constant for pressure ratios 0.05 to approximately 0.45. Typically, the standard deviation of the flow divided by the average of the flow was 0.002.

Listed in table 1 is the orifice diameter d, the flow rate measured by the FM that was calibrated with the Gilibrator ($Q_{FMrefstd}$), the flow rate measured by the current technique ($Q_{CFEVstd}$), and the relative difference between $Q_{FMrefstd}$ and $Q_{CFEVstd}$.

It is important to note that the actual P_{ratio} (P_{dn}/P_{up}) limit was less than that predicted from the above theory. This may be due to imperfections in the machining of the orifice.
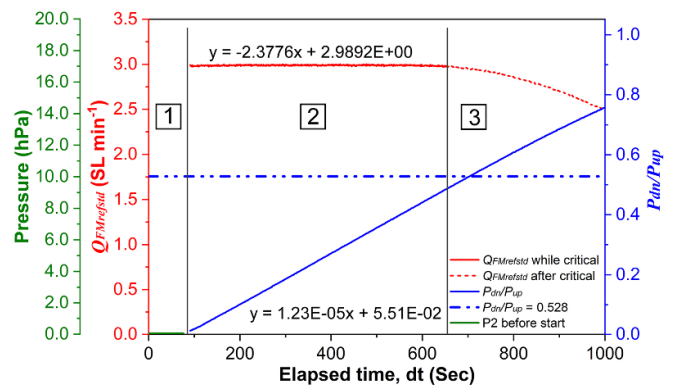
Figure 5. Data using the K6-26-SS orifice. The pressure P_{dn} before allowing flow into the vessel (green), the flow rate $Q_{FMrefstd}$ (red) while allowing flow into the vessel, and the pressure ratio ($P_{ratio} = P_{dn}/P_{up}$) (blue) vs elapsed time dt.

Probably, though, it is due to the fact that the Reynolds number (Re) was less than 30 000 and so the equation which predicted when choked flow will cease (equation (1)) cannot provide accurate, precise values. Predicting an accurate value of P_{ratio} (at which to stop data logging) computed from equation (1) is not all that important, since this value is only used to give an approximate point. The best technique is simply to watch for when the flow as indicated by the FM$_{ref}$ dropped by 1% or 2% and then terminate data logging 60 s or so after that. This usually happened when P_{ratio} (P_{dn}/P_{up}) approached 0.45. Even though data might be logged for another 60 s or so, only data for when the FM$_{ref}$ gave constant readings should be used.

5. Validation of the CFEV method using metal plate orifices

Figure 6 shows the results of comparing the flow past PT A ($Q_{FMrefstd}$) (figure 1) as measured by the FM$_{ref}$ (calibrated in the traditionally accepted way using a Gilibrator and figure 2) and as measured using the $Q_{CFEVstd}$ method using a set of metal plate orifices. These completely different methods agree to within 1%.

6. Needle valves as the CFRs

Some labs may not have (nor wish to purchase) metal plate orifices for the purpose of calibration. Also, choked flow through
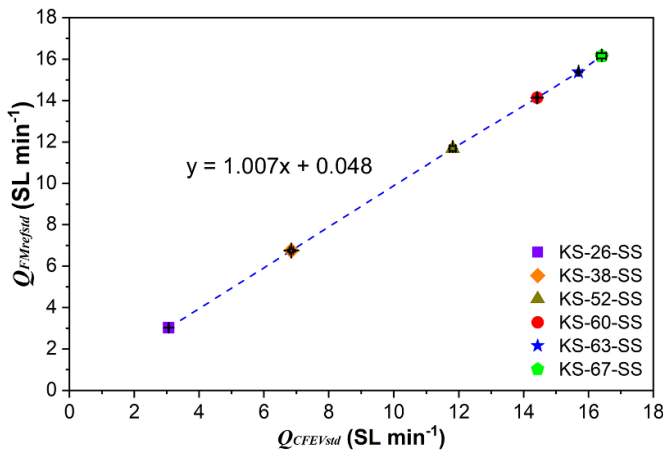
Figure 6. The measured flow rate $Q_{FMrefstd}$ vs the computed flow rate $Q_{CFEVstd}$ for six different orifices. For each data point, there were three trials. The vertical error bars were taken from the standard deviations of the average readings and they are too small to be seen.

an orifice of a particular, fixed diameter will result in only one choked flow rate. If it is desired to use the CFEV method for the purpose of calibration where many different flow rates can be tested without purchasing many different orifice plate sizes, using a needle valve is an easy and viable alternative. Needle valves allow for the precise control of choked flow rates and exist on-hand in many laboratory settings.

Experiments were performed whereby the metal plate orifices were replaced by commonly available needle valves. Table 2 provides a list of the needle valves used in this study and some of their characteristics. The orifice diameter is the actual diameter (d) of the hole into which the needle inserts, listed in the manufacturer's catalogue. Due to the nature of needle valves, the flow of gas through the orifice of the valve may not be compressed to $\beta \leqslant 0.2$, and therefore equation (1) may not be valid. However, as stated previously, the best technique is to simply discontinue data logging a minute or so after when (P_{dn}/P_{up}) approaches 0.45 and/or $Q_{FMrefstd}$ falls by about 1%. Then only use the data for when $Q_{FMrefstd}$ was constant.

7. Validation of the CFEV method using needle valves

Needle valves were used in place of the metal plate orifices as the CFR and plots entirely similar to figure 5 were obtained. Trials were performed with the gas passing through the needle valve in the direction recommended by the valve manufacturer (FWD) and also in the reverse direction (REV). The manufacturer's recommended flow direction is specified (it seems) so that when the valve is closed, there is no gas pressure on the valve stem packing (and hence the likelihood of a leak is minimized), since the needle part has closed off the orifice. Figures 7 and 8 show the $Q_{FMrefstd}$ vs $Q_{CFEVstd}$ for nine different, commonly available needle valves.

When tested in the forward orientation (FWD), for eight of the nine needle valves tested, the agreement between the

Gilibrator calibrated FM ($Q_{FMrefstd}$) and the calculated flow rate using the CFEV method ($Q_{CFEVstd}$) was within 1%. The Whitey valve with 1/8″ ends showed a higher percent error than the rest. Perhaps this is because this valve comes closer to violating the $\beta \leqslant 0.2$ requirement. When the valves were tested in the reverse orientation (REV), five showed an error of 1% or less (when rounded to two digits), and the remaining four showed an error of less than 2%.

8. Testing using multiple flow rates per vessel evacuation/refilling

In order to perform a calibration faster, a needle valve can be used and simply adjusted to several different positions during one vessel refilling. To ensure reliable measurement statistics, we recommend recording at least 45 s of data at each needle valve setting. Or, alternatively, let the P_{dn} rise be 50 times the noise level in the pressure transducer P_{dn}. Figure 9 shows $Q_{FMrefstd}$ and P_{dn} vs dt for when a Swagelok SS-1RS6 needle valve was used and adjusted to four different settings during one vessel refilling. Figure 10 shows the resulting $Q_{FMrefstd}$ vs $Q_{CFEVstd}$ values. It could very well be that even more than four settings of the needle valve are attainable, but we confined ourselves to this to simply show the possibility.

9. Calibrating a FM using gases other than air

Using the CFEV method to calibrate a FM for a gas other than air will now be discussed. For a given CFR, the apparatus of figure 1 is used to measure the dP_{dn}/dt and equation (5) is used to compute $Q_{CFEVstd}$. For each CFR setting, the average V_{fm} is obtained and the plot of $Q_{CFEVstd}$ vs V_{fm} is constructed, yielding the calibration of the FM using the CFEV method for this new gas.

If the goal is to actually compare the two calibrations (Q_{GILstd} vs V_{fm} and $Q_{CFEVstd}$ vs V_{fm}) using the different gas, it is necessary to also calibrate the FM (figure 2 with the Gilibrator) with the alternative gas (equation (7)). A new calibration formula is inserted into the LabVIEW program (LV01) relating $Q_{FMrefstd}$ vs output voltage of the FM (V_{fm}). Clearly the Gilibrator must be used as part of figure 2 and then a routine calibration of the FM is performed using the CFEV method.

Both argon and CO_2 were used as an alternative gas and a calibration with them was achieved as in figures 1 and 2. A comparison of the soap film FM calibrated FM (Q_{GILstd}) was made against the CFEV method ($Q_{CFEVstd}$). The results, shown in figure 11, show the agreement between Q_{GILstd} and $Q_{CFEVstd}$ is better than 0.1% for CO_2 and approximately 2% for argon.

## 10. Calibrating a FM with various inlet pressures to the CFR

The question arises as to whether this CFEV technique will work if the inlet pressure P_{up} at the entrance to the CFR is varied to something significantly different from room air pressure. Referring to figure 1 it is apparent that by increasing the pressure provided by the pressure regulator of the source gas

**Table 2.** Characteristics of various needle valves.

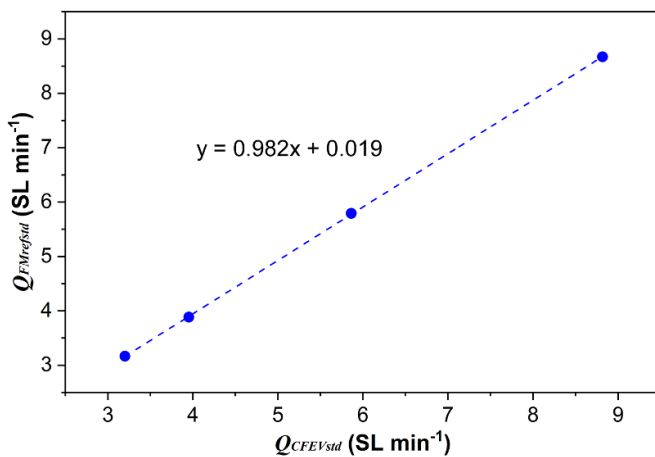| Manufacturer	Model number	Ends (inch (mm))	Orifice diameter, d (inch (mm))	Slope-FOR	Intercept-FOR	Slope-REV	Intercept-REV
Whitey	SS-B-1KS4	1/4 (6.35)	Unknown	1.0003	0.0600	0.9973	−0.0145
Whitey	SS-31RS4	1/4 (6.35)	0.172 (4.37)	1.0065	0.0524	1.0201	−0.1289
Nupro	SS-4UW	1/4 (6.35)	0.172 (4.37)	0.9996	0.1466	0.9767	0.0553
FloLok	AB414	1/4 (6.35)	0.172 (4.37)	0.9986	0.1093	0.9885	0.0081
Swagelok	SS-1RS6	3/8 (9.52)	0.25 (6.35)	1.0068	0.0768	0.9945	−0.0436
Whitey	SS-7RS8	1/2 (12.7)	0.437 (11.1)	1.0005	0.1151	0.9798	0.1188
Whitey	Illegible	1/8 (3.18)	Unknown	1.0279	−0.0290	0.9889	0.0506
Whitey	SS-1RS4	1/4 (6.35)	0.172 (4.37)	1.0065	0.0775	0.9845	0.0956
Whitey	SS-12NKRS8	1/2 (12.7)	0.437 (11.1)	1.007	0.240	1.0025	0.153
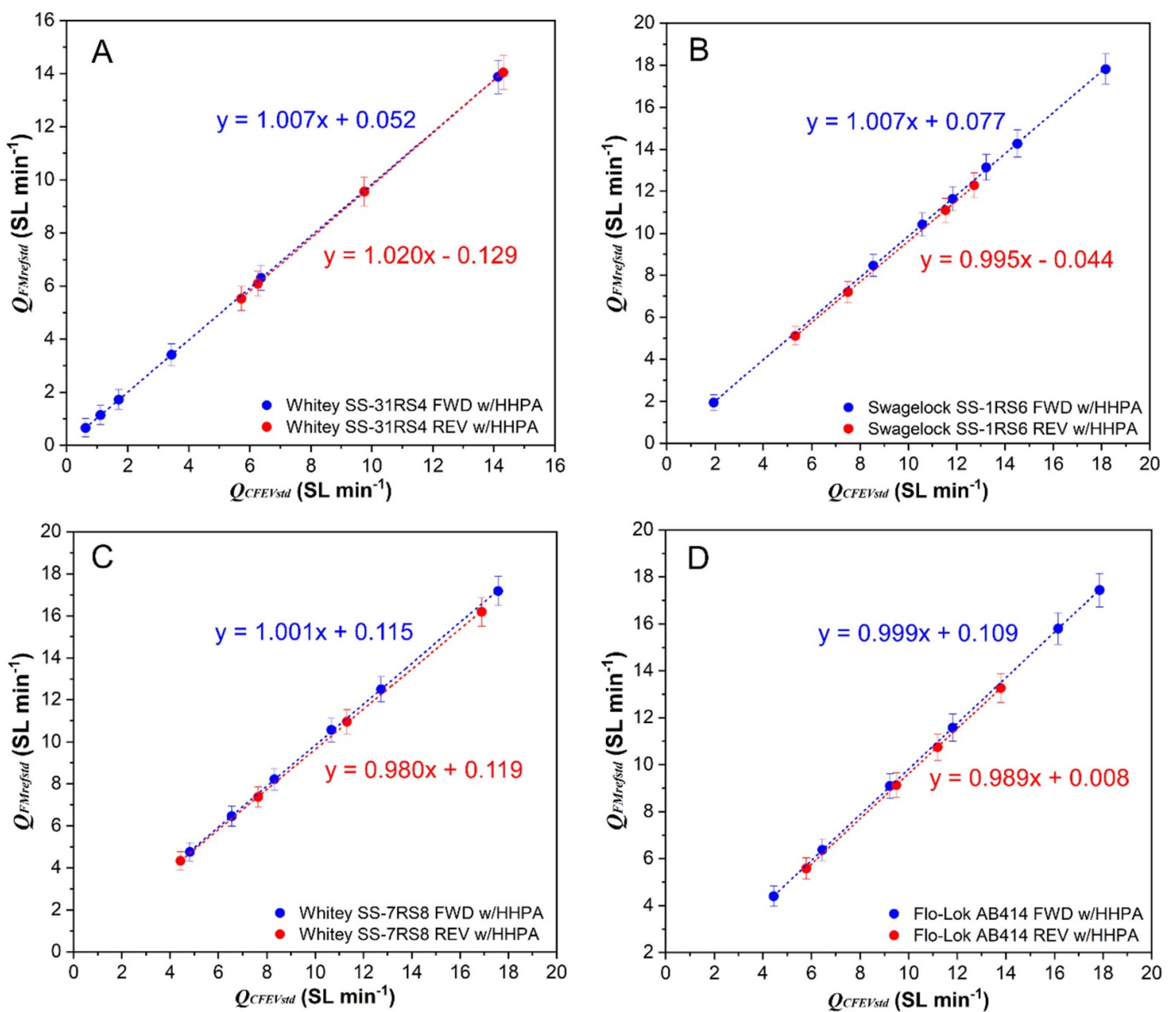
Figure 7. The Q_{FMrefstd} is plotted against the Q_{CFEVstd} for several models of needle valves tested. Note that results are shown for both the FWD and REV direction of flow. (A Whitey SS-31RS4, B Swagelok SS-1RS6, C Whitey SS-7RS8, D Flo-Lok AB414).
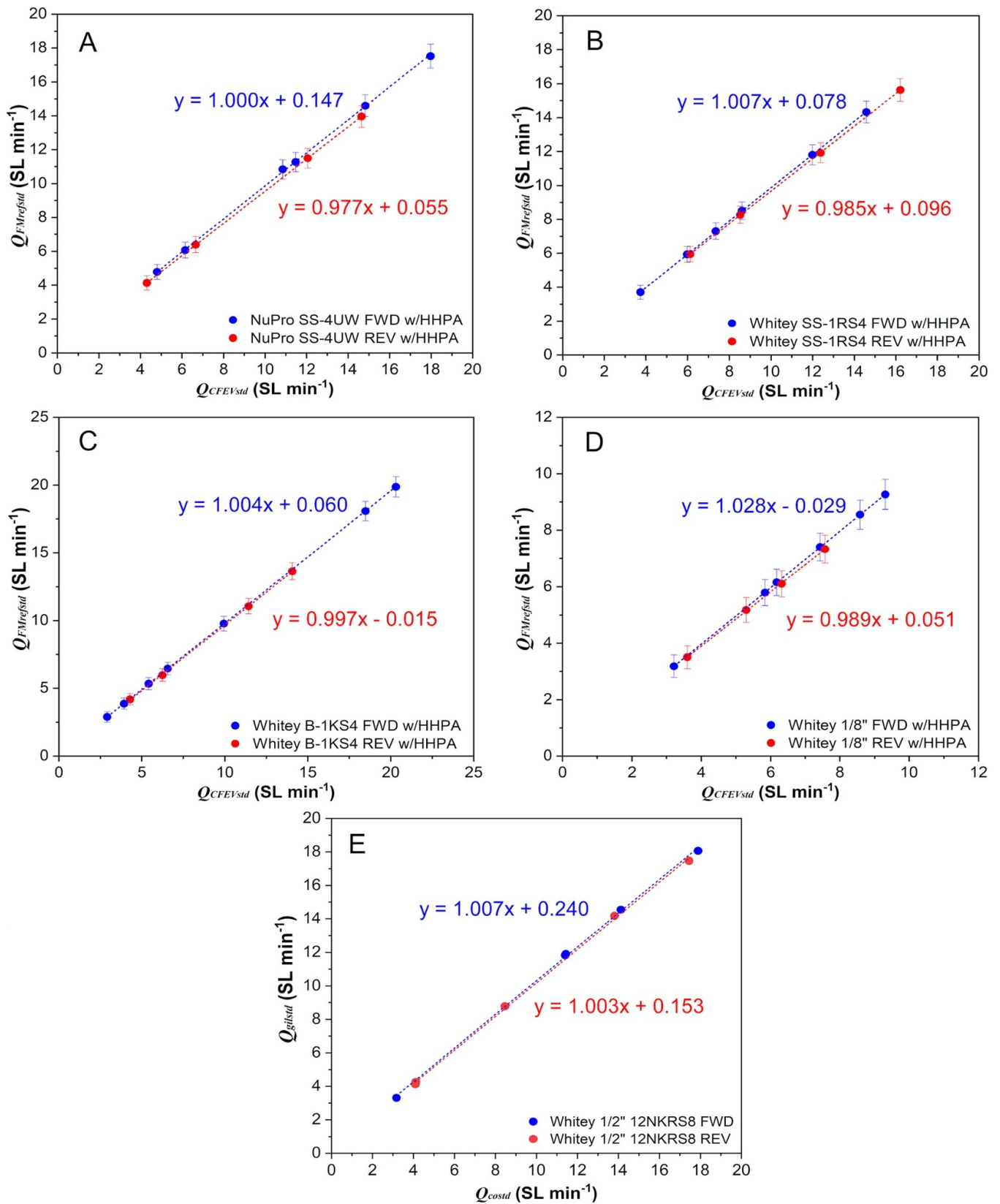
Figure 8. The Q_{FMrefstd} is plotted against the Q_{CFEVstd} for several more models of needle valves tested. Note that results are shown for both the FWD and REV direction of flow. (A NuPro SS-4UW, B Whitey SS-1RS4, C Whitey B-1KS4, D Whitey 1/8″, and E Whitey SS-12NKRS8).
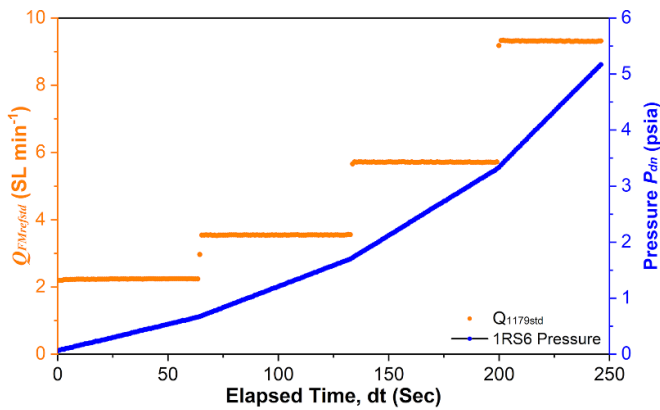
Figure 9. This plot shows the flow rate $Q_{FMrefstd}$ (red) and the pressure P_{dn} (blue) vs elapsed time dt for an experiment wherein four different flow rates for a single evacuation/refilling of the vessel were achieved. Compressed air was used and the needle valve was in FWD orientation.

Figure 11. Q_{GILstd} vs $Q_{CFEVstd}$ using argon and CO_2 as the gas. The vertical error bars are on the points but are too small to be seen.
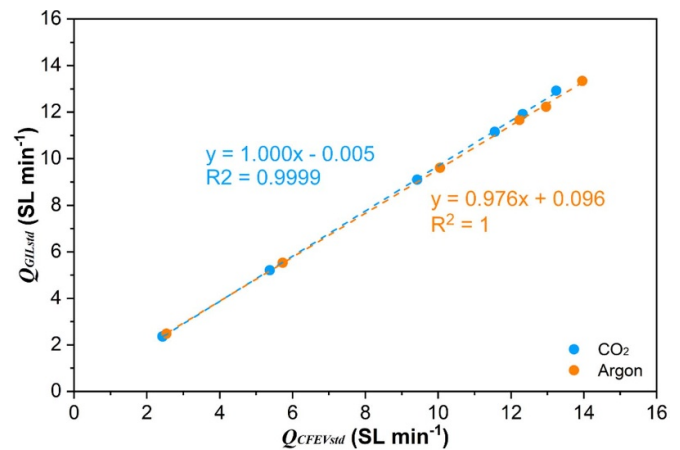

Figure 10. $Q_{FMrefstd}$ vs $Q_{CFEVstd}$ for four different flow rates for one vessel evacuation/refilling. The valve used was the Swagelok MN SS-1RS6.

Figure 12. The gas flow past PT A as measured by the Gilibrator calibrated FM ($Q_{FMrefstd}$) and the gas flow as measured by the CFEV method ($Q_{CFEVstd}$) as the pressure to the inlet of the choked flow restriction (P_{up}) is varied away from 1 atm.

(the tank of compressed air or some alternative gas) and limiting the flow out of the rotameter (Q_2), the pressure at the inlet of the FM and also the pressure at the CFR (P_{up}) can be increased.
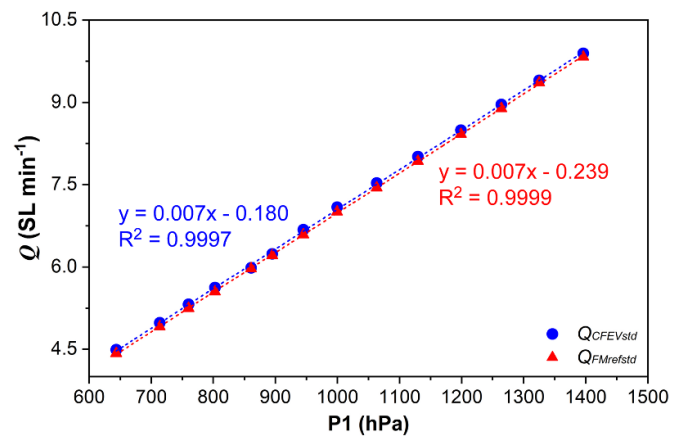
Alternatively, by closing the valve at Q_2 and limiting the flow of the gas in, pressures less than 1 atm at the inlet of the CFR can be imposed. Figure 12 shows that the two methods (Gilibrator calibrated FM and CFEV) agree very well. Ambient pressure in our lab was about 960 hPa. Hence, the CFEV technique works well even when the inlet pressure P_{up} at the entrance to the CFR differs significantly from room air pressure.

11. Ultimate accuracy

Note the relationship between $Q_{FMrefstd}$ and the FM output signal (V_{fm}) shown in figure 3. Several points should be highlighted. First it is obvious from figure 3 that the FM signal (V_{fm}) is dependent upon the properties of the gas used. Secondly, when one calibrates a FM using the Gilibrator and

any gas, e.g. air, one does not actually arrive at a true calibration for that FM and that gas. In actuality, one has arrived at a calibration for a gas mixture of perhaps 97% that gas and 3% water vapor. This is because the Gilibrator adds a small amount of gas in the form of water vapor to the incoming gas. That is inescapable. The fact that the calibration of the FM is different for the three different gases—air, argon, and CO_2, means that a true calibration for any gas, say gas X, will not be achieved when using the Gilibrator, because one is actually using gas X plus a small amount of water vapor, gas Y.

One could put the Gilibrator downstream of the FM to be tested, but that would not actually be any better. This is because then the FM would actually have a smaller gas flow through it than the Gilibrator, because the water vapor would only be added after the FM when the gas passes through the Gilibrator. Furthermore, the amount of water vapor added to the gas in the Gilibrator is dependent upon the flow rate. Separate experiments showing this have been performed and will be detailed in a later paper.

The beauty of the CFEV method, however, is that it does not suffer from this problem. When a FM is calibrated with a certain gas using the CFEV technique, then it is truly calibrated for that gas.

12. Precision of the CFEV method

12.1. The method of quadrature

The error bars on the plots in this manuscript were obtained using the method of quadrature:

$$
\delta g\left(x, y, z, \ldots\right) = \sqrt{\left(\delta x\left(\frac{\partial g}{\partial x}\right)\right)^2 + \left(\delta y\left(\frac{\partial g}{\partial y}\right)\right)^2 + \left(\delta z\left(\frac{\partial g}{\partial z}\right)\right)^2 + \ldots}
$$

$$(10)$$

The uncertainties in the readings taken directly from the Gilibrator (Q_{GILstd}) and the uncertainties in the readings from the FM$_{\mathrm{ref}}$ (Q_{FMrefstd}) as taken by the National Instruments USB-6009/laptop computer are treated separately in the following.

12.2. Uncertainty in Q$_{FMrefstd}$

Applying equation (10) to equation (7) for the uncertainty in Q_{FMrefstd}

$$
\delta Q_{\mathrm{FMrefstd}}\left(M, V_{\mathrm{fm}}\right) = \sqrt{\left(\delta M\left(\frac{\partial Q_{\mathrm{FMrefstd}}}{\partial M}\right)\right)^2 + \left(\delta\left(V_{\mathrm{fm}}\right)\left(\frac{\partial Q_{\mathrm{FMrefstd}}}{\partial\left(V_{\mathrm{fm}}\right)}\right)\right)^2}.
$$

$$(11)$$

The δM is the range in slopes of the FM calibration (taken from five different calibrations) in equation (7). Also

$$
\frac{\partial Q_{\mathrm{FMrefstd}}}{\partial M} = V_{\mathrm{fm}} \tag{12}
$$
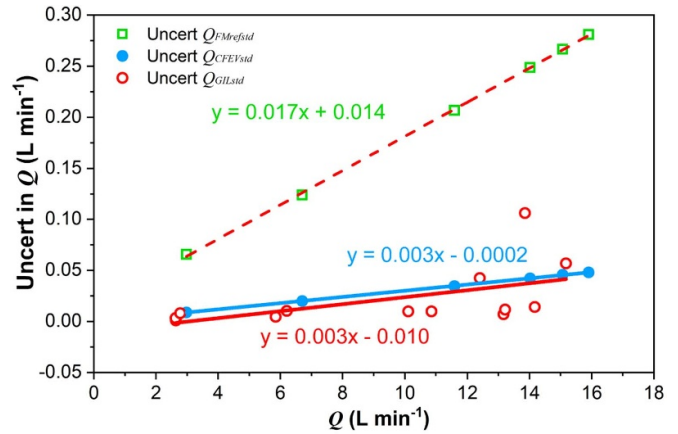
which is a function of the flow rate. The variation in the MFM signal as measured by the USB-6009 even at a fixed flow rate, $\delta\left(V_{\mathrm{fm}}\right)$ is fairly constant, and was taken as 0.01 V_{dc}. And finally

$$
\frac{\partial Q_{\mathrm{FMrefstd}}}{\partial\left(V_{\mathrm{fm}}\right)} = M_{\mathrm{FMrefstd}} \tag{13}
$$

which is a constant with value 4 (L min^{-1} volt^{-1}).

12.3. Uncertainty in Q$_{CFEVstd}$

Applying equation (10) to equation (9) for the uncertainty in Q_{CFEVstd}

Figure 13. Uncertainty in Q_{FMrefstd}, Q_{GILstd} and Q_{CFEVstd} vs the flow rate of each of them.

$$
\delta Q_{\mathrm{CFEVstd}}\left(V, \frac{\mathrm{d}P}{\mathrm{d}t}\right) = \sqrt{\left(\delta V\left(\frac{\partial Q_{\mathrm{CFEVstd}}}{\partial V}\right)\right)^2 + \left(\delta\left(\frac{\mathrm{d}P}{\mathrm{d}t}\right)\left(\frac{\partial Q_{\mathrm{CFEVstd}}}{\partial\left(\frac{\mathrm{d}P}{\mathrm{d}t}\right)}\right)\right)^2}
$$

$$(14)$$

$$
\frac{\partial Q_{\mathrm{CFEVstd}}}{\partial V} = 0.05517 \cdot \left(\frac{\mathrm{d}P}{\mathrm{d}t}\right) \tag{15}
$$

$$
\frac{\partial Q_{\mathrm{CFEVstd}}}{\partial\left(\frac{\mathrm{d}P}{\mathrm{d}t}\right)} = 0.05517 \cdot V. \tag{16}
$$

Note that $\mathrm{d}P/\mathrm{d}t$ is a function of the flow rate.

12.4. Uncertainty in Q$_{GILstd}$

The uncertainties in the Gilibrator readings (Q_{GILstd}) were taken from the standard deviations from experiments done with the metal plate orifices.

12.5. Uncertainties compared

The data for the metal plate orifices served as a convenient source of data from which to obtain values for equation (11) through equation (16). This then results in the data of figure 13, which displays the uncertainty in Q_{FMrefstd}, Q_{GILstd}, and Q_{CFEVstd} as functions of the flow.

It is seen that the uncertainties in the CFEV method and those of the readings taken directly from the Gilibrator are comparable. Also, both of these are considerably less than the uncertainties of the reading from the FM$_{\mathrm{ref}}$/USB-6009.

Thus, the CFEV and the Gilibrator are about six times more precise in measuring a flow than measuring that flow with the FM$_{\mathrm{ref}}$ which for us was the MKS$_{1179}$/MKS247/USB-6009.

It is common practice to require that when calibrating any device, the uncertainty in the standard should be no greater

than one fourth of the uncertainty of the unit under test. Inspection of figure 13 shows that this criterion is easily attained. Thus, the Gilibrator technique and the CFEV technique can legitimately be used as standards for calibrating mass and VFMs.

13. Calibration of a MFM using the CFEV method

MFMs provide the gas flow in units of standard liters min^{-1} (SL min^{-1}). To use this CFEV method to calibrate a MFM, one uses the output voltage (V_{fm}) from the MFM as the *x* value and the value from equation (9) as the *y* value for the calibration curve. For example, see figure 3. If the output voltage (V_{fm}) is not available, then simply use the meter reading from its front panel as the *x* value.

14. Calibration of a VFM using the CFEV method

Some FMs do not provide the flow in standard liters/min (SL min^{-1}), but rather the actual flow rate (L min^{-1}) and are termed VFMs. These include the Gilibrator, a rotameter, and those that measure the pressure drop across a laminar flow element or a capillary. To calibrate these VFMs using the CFEV technique, the same setup as before is used, i.e. figure 1. Then equation (9) again provides the $Q_{CFEVstd}$ (SL min^{-1}) values. Equation (6) is rearranged to compute the flow rate that should be registered by the VFM, as shown in equation (17). We note that the direct reading of both the Gilibrator and any VFM provides the actual flow in liters min^{-1} (L min^{-1}):

$$Q_{VFM}\left(1\,min^{-1}\right) = Q_{CFEVstd} \cdot \left(SL\,min^{-1}\right) \cdot \left(\frac{P_{std}}{P_g}\right) \cdot \left(\frac{T_g}{T_{std}}\right).$$ (17)

Note that the present technique provides the flow rate in standard liters/min (SL min^{-1}) ($Q_{CFEVstd}$ from equation (9)), whereas the Gilibrator's direct reading is in actual liters/min (L min^{-1}) but can be converted to standard liters/min (SL min^{-1}) by equation (6) (Q_{GILstd}). What matters is the parameter or variable as manifested by the units, SL min^{-1} or L min^{-1}.

15. Calibrating an MFM using the CFEV method—final comparison

To actually calibrate any FM (MFM or VFM) using the CFEV method, one must plot the flow rate $Q_{CFEVstd}$ vs the FM's output signal (V_{fm}). In figure 14 both Q_{GILstd} and $Q_{CFEVstd}$ are plotted against the V_{fm}, not one against the other. This particular plot utilized the Swagelok SS-1RS6 needle valve and compressed air. Notice that the curves agree quite well.
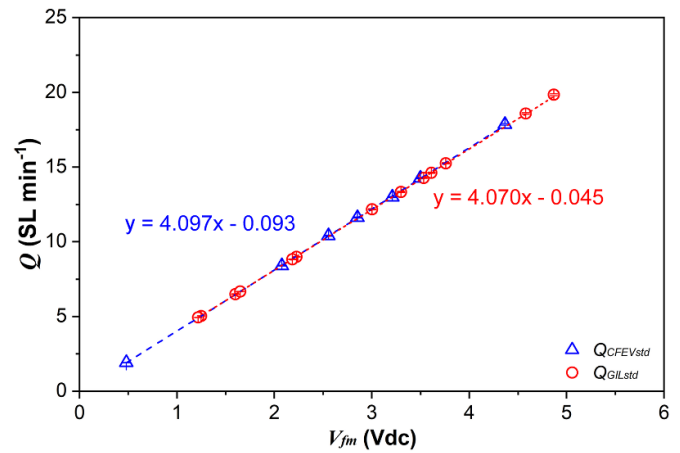
Figure 14. The $Q_{CFEVstd}$ and Q_{GILstd} are plotted against the FM output signal (V_{fm}). The agreement is quite good. This trial involved the use of a Swagelok SS-1RS6 valve as the CO.

16. Conclusions

This paper introduces a simple, yet accurate technique for in-house calibration of FMs (mass and volumetric) even under harsh environmental conditions such as encountered during field measurement campaigns. This technique directly yields the mass flow rate (not volumetric flow rate), which, to the present authors, seems more desirable. However, the volumetric flow rate is easily calculated from that. This technique is shown to give excellent agreement with the accepted soap film flow meter (Gilibrator) technique. This technique involves using an evacuated vessel of known volume (V_{vess}) and a CO to provide choked flow. The evacuated vessel is allowed to fill with gas passing through the CO (a metal plate orifice or a needle valve). The ideal gas law is differentiated with respect to time, holding the volume and temperature constant. Thus, the time rate of change of the number of moles (or flow rate) in the controlled volume (V_{vess}) is directly proportional to the time rate of change of the absolute pressure in the vessel (dP_{dn}/dt). As long as the orifice is maintained at criticality, the flow through the orifice is quite constant, allowing one enough time to take an accurate average reading of the FM output signal (V_{fm}). During that time, the gas pressure in the vessel is monitored with time. The plot of pressure in the vessel P_{dn} vs time is made and the slope of that (dP_{dn}/dt) is obtained and used in the differentiated ideal gas law to compute the gas flow rate ($Q_{CFEVstd}$). The Gilibrator can also be installed just upstream of the FM$_{ref}$ and provide readings of the flow rate (Q_{GILstd}). The three readings of $Q_{CFEVstd}$, Q_{GILstd} and $Q_{FMrefstd}$ are compared and are in excellent agreement (typically 1%). This method was shown to work for metal plate orifices and commonly available needle valves over the range of 2–20 SL min^{-1}. In order to achieve faster FM calibrations, the needle valve can be adjusted to several different settings and provide as many as four calibration points with just one vessel evacuation/refilling (62.7 l volume). The method has been shown to work with compressed air, Argon, and CO_2. The method has

also been shown to work with varying pressures from 650 hPa to 1400 hPa at the inlet of the CO. The uncertainty in the calculated flow rate from this technique is almost identical to the uncertainty in the direct readings from the Gilibrator. Furthermore, both of these uncertainties are approximately 1/6 of the uncertainty in the reading of the electronic FM (calibrated earlier with the Gilibrator), making this technique quite worthy of being a calibration technique for mass and VFMs. The writers propose that the accuracy/precision of this technique is limited only by the accuracy/precision of the V_{VESS} measurement and the accuracy/precision of the time rate of change of the vessel pressure measurement.

Data availability statement

The data that support the findings of this study are available upon reasonable request from the authors.

Acknowledgments

Author contributions

M B T and D E H designed the study. M B T and S C A developed the LabVIEW code. M B T, N A, C H, D S, T G, and W L performed the measurements. M B T, N A, C H, D S, T G and W L analyzed the data. M B T and N A prepared the figures. W L prepared the plots. M B T wrote the initial manuscript and subsequent revisions with contributions from O S, D E H, S C A, W L, N A, C H, D S, T G, and P D W.

Conflict of interest

The authors declare that they have no conflict of interest.

ORCID iD

Max B Trueblood ⬤ https://orcid.org/0000-0003-4483-2346

References

Baker R C 2016 *Flow Measurement Handbook* 2nd edn (Cambridge: Cambridge University Press) (https://doi.org/10.1021/es301898u)

Bulzan D *et al* 2010 Gaseous and particulate emissions results of the NASA alternative aviation fuel experiment (AAFEX) *Am. Soc. Mech. Eng.* **2** 1195–207

Christie S, Raper D, Lee D S, Williams P I, Rye L, Blakey S, Wilson C W, Lobo P, Hagen D E and Whitefield P D 2012 Polycyclic aromatic hydrocarbon emissions from the combustion of alternative fuels in a gas turbine engine *Environ. Sci. Technol.* **46** 6393–400

Cunningham R G 1951 Orifice meters with supercritical compressible flow *Trans. ASME* 625–38

European Aviation Safety Agency (EASA) 2015 *International Civil Aviation Organization Aircraft Engine Emissions DataBank* (Cologne, Germany: European Aviation Safety Agency) (available at: www.easa.europa.eu/easa-and-you/environment/icao-aircraft-engine-emissions-databank)

Hagen D E, Paladino J, Whitefield P D, Trueblood M B and Lilenfeld H V 1997 Airborne and ground based jet engine aerosol emissions sampling during two NASA field projects: SUCCESS and SNIF *J. Aerosol. Sci.* **28** 67–8

Hagen D E, Trueblood M B and Whitefield P D 1992 A field sampling of jet exhaust aerosols *Particul. Sci. Technol.* **10** 53–63

Hagen D, Whitefield P, Paladino J, Schmid O, Schlager H and Schulte P 1999 Atmospheric aerosol measurements in the North Atlantic flight corridor during project POLINAT-2 *J. Aerosol. Sci.* **30** 161–2

Johnson A N, Espina P I, Mattingly G E, Wright J D and Merklet C L 1998 Numerical characterization of the discharge coefficient in critical nozzles *1998 NCSL Workshop & Symp., Session 4E* pp 407–22

Johnson A N and Wright J D 2009 Gas flowmeter calibrations with the 26 m3 PVTt standard, NIST Special Publication 1046

Jones F E and Harris G L 1992 ITS-90 density of water formulation for volumetric standards calibration *J. Res. Natl Inst. Stand. Technol.* **97** 335–40

Kegel T 1995 Uncertainty analysis of a volumetric primary standard for compressible flow measurement *3rd Int. Symp. of Fluid Flow Measurement* (*San Antonio, TX, USA*)

Kinsey J *et al* 2012 Determination of the emissions from an aircraft auxiliary power unit (APU) during the Alternative Aviation Fuel Experiment (AAFEX) *J. Air Waste Ma.* **62** 420–30

Kinsey J, Yuanji D, Williams D and Russell L 2010 Physical characterization of the fine particle emissions from commercial aircraft engines during the Aircraft Particle Emissions eXperiment (APEX) 1-3 *Atmos. Environ.* **44** 2146–56

Lashkari S and Kruczek B 2008 Development of a fully automated soap flowmeter for micro flow measurements *Flow Meas. Instrum.* **19** 397–403

Lee D S *et al* 2010 Transport impacts on atmosphere and climate *Aviation Atmos. Environ.* **44** 4678–734

Lee D S, Fahey D W, Forster P M, Newton P J, Wit R C N, Lim L L, Owen B and Sausen R 2009 Aviation and global climate change in the 21st century *Atmos. Environ.* **43** 3520–37

Levine P D 2010 A new approach to gas flow calibration *Measurement* **43** 1644–8

Levy J I, Woody M, Baek B H, Shankar U and Arunachalam S 2012 Current and future particulate-matter-related mortality risks in the United States from aviation emissions during landing and takeoff *Risk Anal.* **32** 237–49

Lobo P *et al* 2012 Impact of alternative fuels on emissions characteristics of a gas turbine engine-part 1: gaseous and particulate matter emissions *Environ. Sci. Technol.* **46** 10805–108011

Lobo P, Christie S, Khandelwal B, Blakey S G and Raper D W 2015 Evaluation of non-volatile particulate matter emission characteristics of an aircraft auxiliary power unit with varying alternative jet fuel blend ratios *Energ. Fuel.* **29** 7705–11

Lobo P, Hagen D E and Whitefield P D 2011 Comparison of PM emissions from a commercial jet engine burning conventional, biomass, and Fischer-Tropsch fuels *Environ. Sci. Technol.* **45** 10744–9

Mascomani R and Chandapillai J 2017 *Design Aspects of PVTt Primary Standard, Uncertainty and Traceability of 50 Bar Calibration and Test Facility, Flotek.g Global Conf. & Exhibition*

McNaught A D and Wilkinson A 1997 *Compendium of Chemical Terminology, the Gold Book* 2nd edn (Hoboken, NJ: Blackwell Science) (https://doi.org/https://doi.10.1351/goldbook.S05921)

Moore R H *et al* 2017 Take-off engine particle emission indices for in-service aircraft at Los Angeles International Airport *Sci. Data* **4** 170198

Nakao S, 2006 Development of the PVTt system for very low gas flow rates *Flow Meas. Instrum.* **17** 193–200

Paladino J, Hagen D E, Whitefield P D, Hopkins A R, Schmid O, Wilson M R, Schlager H and Schulte P 2000 Observations of particulates within the North Atlantic flight corridor: POLINAT II Sep–Oct 1997 *J. Geophys. Res.* **105** 3719–26

Paton R 2005 Calibration and standards in flow measurement *Handbook of Measuring System Design* (Hoboken, NJ: Wiley) pp 1258–9

Perry R H and Chilton C H 1973 *Chemical Engineers' Handbook* 5th edn (New York: McGraw Hill Book Company) pp 5–12

Ross M N *et al* 2000 Observation of stratospheric ozone depletion associated with Delta II rocket emissions *Geophys. Res. Lett.* **27** 2209–12

Ross M N, Whitefield P D, Hagen D E and Hopkins A R 1999 *In situ* measurement of the aerosol size distribution in stratospheric solid rocket motor exhaust plumes *Geophys. Res. Lett.* **26** 819–22

Schmid O, Trueblood M B, Gregg N, Hagen D E and Whitefield P D 2010 Sizing of aerosol in gases other than air using a differential mobility analyzer *Aerosol. Sci. Tech.* **36** 351–60

Schulte P, Schlager H, Ziereis H, Schumann U, Baughcum S L and Deidewig F 1997 NO$_x$ emission indices of subsonic long-range aircraft at cruise altitude: *in situ* measurements and predictions *J. Geophys. Res.-Atmos.* **102** 21431–42

Trueblood M B, Lobo P, Hagen D E, Achterberg S A, Liu W and Whitefield P D 2018 Application of a hygroscopicity tandem differential mobility analyzer for characterizing PM emissions in exhaust plumes from an aircraft engine burning conventional and alternative fuels *Atmos. Chem. Phys.* **18** 17029–45

Waaben J, Stokke D B and Brinklov M M 1978 Accuracy of gas flow meters determined by the bubble meter method *Br. J. Anaesth.* **50** 1251

Waitz I A, Townsend J, Cutcher-Gershenfeld J, Greitzer E and Kerrebrock J 2004 Aviation and the environment *Report to the United States Congress, Partnership for AiR Transportation Noise and Emissions Reduction* (Cambridge, MA: Massachusetts Institute of Technology)

Whitefield P D, Ross M N, Hagen D E and Hopkins A R 1999 Aerosol characterization in rocket plumes *J. Aerosol. Sci.* **30** 215–6

Wright J D 1998c The long term calibration stability of critical flow nozzles and laminar flowmeters *National Conf. of Standards Laboratories Conf. Proc.* (*Albuquerque, NM, USA*) pp 443–62

Wright J D, George E. Mattingly G E, Nakao S-I, Yokoi Y and Takamoto M 1998b Intercomparison tests of a NIST primary standard with a NRLM *Metrologia* **35** 211–21

Wright J D and Johnson A N 2000 Uncertainty in primary gas flow standards due to flow work phenomena *Flomeko 2000-IMEKO TC9 Conf.* (*Salvador, Bahia, Brazil, June, 2000*) pp 4–8

Wright J D, Johnson A N, Moldover M R and Kline G M 2004 Gas flowmeter calibrations with the 34 L and 677 L PVTt standards, NIST Special Publication 250-63 (https://doi.org/10.6028/NIST.SP.250-63)

Wright J D and Mattingly G E 1998a NIST calibration services for gas flow meters, NIST Special Publication 250-49 (https://doi.org/10.6028/NIST.SP.250-49)

Technical Report Documentation Page

1. Report No.	2. Government Accession No.	3. Recipient's Catalog No.

4. Title and Subtitle	5. Report Date
	6. Performing Organization Code

7. Author(s)	8. Performing Organization Report No.

9. Performing Organization Name and Address	10. Work Unit No. (TRAIS)
	11. Contract or Grant No.

12. Sponsoring Agency Name and Address	13. Type of Report and Period Covered
	14. Sponsoring Agency Code

15. Supplementary Notes

16. Abstract

17. Key Words	18. Distribution Statement

19. Security Classif. (of this report)	20. Security Classif. (of this page)	21. No. of Pages	22. Price
Unclassified	Unclassified		

Form DOT F 1700.7 (8-72)   Reproduction of completed page authorized